MODELLING AND CONTROL OF COMBINED COOLING AND ANTISOLVENT CRYSTALLIZATION PROCESSES

Z. K. Nagy,[†1] M. Fujiwara,[‡] and R.D. Braatz[‡]

[†]*Department of Chemical Engineering, Loughborough University,*

Loughborough, LE11 3TU, United Kingdom

[‡]*Department of Chemical and Biomolecular Engineering,*

University of Illinois at Urbana-Champaign, Urbana, Illinois, 61801, USA

Abstract

Although for decades nearly all pharmaceuticals have been purified by crystallization, there have been a disproportionate number of problems associated with the operation and control of these processes. This paper provides an overview of the recent advances in model-based and model-free (direct design) approaches to control the crystallization of pharmaceuticals, treating both antisolvent and cooling crystallization. A model-based combined technique which simultaneously controls the antisolvent addition rate and the cooling profile is presented. A population balance model of the combined cooling-antisolvent addition system is developed and a moments model is used in optimal control strategies with various objective functions. The simulation and experimental results show the advantages of the combined approach.

Keywords: crystallization control, optimal control, process analytical technology

[1] Corresponding author: Z.K.Nagy@lboro.ac.uk

1. INTRODUCTION

Batch crystallization is among the oldest unit operations in the chemical industry. Despite this long history and the widespread application of crystallization, there are still a disproportionate number of problems associated with the understanding and control of the process. These problems have become highly important in recent years as an increased interest has been directed towards crystallization of pharmaceuticals and proteins, which have additional complications compared to the inorganic crystallizations studied extensively before (Fujiwara et al., 2005). The major concern in the pharmaceutical industry is to optimize consistency and quality of the final product while improving productivity if possible. Pharmaceutical manufacture has traditionally been a recipe-based operation, in which the processes are controlled by following operating trajectories in accordance to the specifications submitted for regulatory filings. In recent years the application of experimental design techniques to identify a robust envelope for crystallization operation has become more and more widespread in the pharmaceutical industries. The response surface method can be used to design optimal cooling trajectories (Togkalidou et al., 2001a). However, these approaches usually require many experiments for reliable determination of optimal operating policies which are robust during scale-up. In recent years accurate *in situ* sensors have become available, which are robust enough to be applied in the production environment. This opened the possibility of feedback control-based crystallization design and operation. The new opportunities are well described by the guideline document issued in 2004 by the US Food and Drug Administration (FDA), as part of a broader initiative on current Good Manufacturing Practices (cGMP), which puts a growing emphasis on the development and use of novel technologies based on process analytical technologies (PAT) as a tool for "21st Century Manufacturing" (Birch et al., 2005; Yu et al., 2004) and the development of tailored process control strategies is being recognized as the most important way to prevent or mitigate the risk of producing poor quality products. Recent research has indicated the significant economic potential of using advanced feedback control strategies within the framework of PAT (see Braatz, 2002; Fujiwara et al., 2005; Nagy et al., 2004 and references cited therein), to reduce time-to-market and increase product quality. The new policy adopted by the FDA with the aim to achieve and consistently maintain product quality and performance allows a certain degree of flexibility for changes in operating conditions in the manufacturing process, as opposed to the previously adopted rather restrictive recipe-based operation. This provides a significant potential for implementation of optimal and adaptive control methodologies with real economic benefits associated with better product

quality and reduced waste due to failed batches. Such control algorithms have been implemented at several pharmaceutical companies (e.g., Liotta and Sabesan, 2004; Zhou et al., 2006).

The fundamental driving force for crystallization from solution is the difference in the chemical potential between the solution and the solid phase, which is usually expressed in terms of the closely related supersaturation, which is the difference between the solution concentration and the saturation concentration or some related expression. The size, shape, and solid-state phase of the product crystals are dependent on the supersaturation profile achieved during the crystallization process. Most often supersaturation is created by cooling, evaporation, or antisolvent addition, with the two main technologies used for batch or semi-batch crystallization being the cooling and antisolvent addition, respectively. A significant number of publications deal with each approach separately (Braatz, 2002; Jones, 2002). Optimal temperature profiles have been determined for numerous systems (Rawlings et al., 1993). Although in the pharmaceutical industries the heuristic combination of these two procedures is fairly common, a systematic study of the combined procedure has not been presented in the literature yet.

The paper first presents a comparative overview of the antisolvent and cooling crystallizations and describes how to systematically combine the two technologies both in the direct design (model-free) and the model-based control framework. Then the model-based combined approach is presented and evaluated through both simulations and experiments. The novelty of the proposed model-based approach is that an optimal control problem is formulated that simultaneously optimizes the antisolvent addition rate and temperature profile in order to improve the quality of the product. The model system used in the evaluation studies is lovastatin (an active pharmaceutical ingredient, API, used as hypolipidemic agent in drugs) in acetone-water mixture. Solubility experiments have been performed using attenuated total reflection-Fourier transform infrared (ATR-FTIR) spectroscopy, in order to determine the solubility of the product as a function of the temperature and antisolvent concentration (Jones and Teodossiev, 1988; Fuijiwara et al., 2002; Feng and Berglund, 2002; Liotta and Sabesan, 2004; Zhou et al., 2006). The solubility of lovastatin is fit with an artificial neural network as a function of temperature and acetone/water ratio. A population balance model for the antisolvent crystallization has been developed and solved using the method of moments. The model with the experimentally determined solubility data was used to obtain optimal control strategies via simultaneous cooling and antisolvent addition considering different productivity and quality objectives. The combined approach is compared to the techniques in which antisolvent addition or cooling is used independently.

2. MODEL-BASED AND DIRECT DESIGN APPROACHES FOR ANTISOLVENT AND COOLING CRYSTALLIZATION SYSTEMS

By far one of the most common batch crystallization approaches is cooling crystallization in which supersaturation is generated by decreasing the temperature. The rate in which the temperature is decreased influences the level of supersaturation, and can be used as a control variable to achieve desired solid-state properties. The main advantage of the cooling crystallization is that no additional raw material (e.g., antisolvent) is needed, which could create additional problems in product purity and increase operating and capital costs. Crystallization from solution using an antisolvent (often called precipitation, however this term more correctly should be used when reaction is involved) is commonly applied in the pharmaceutical industry, in which solute is crystallized from a primary solvent by the addition of a second solvent (antisolvent) in which the solute is relatively insoluble. Typically, a solution of the solute in a solvent, which is often saturated or close to saturation, is initially formed. Then, an antisolvent that is miscible with the primary solvent is added. Sometimes multiple solvents or antisolvents are used, to produce a sharper solubility curve or to produce a more desirable crystal shape or polymorph (crystal structure).

When the antisolvent is added to the solution, the solute crystallizes due to the reduction in solubility. The main advantages of the antisolvent crystallization include the use of low operating temperature, which is important for thermally sensitive products. Another advantage is that the solvent activity also changes significantly, hence this approach can have more profound effect on the crystal morphology or polymorphic form than in the case of the cooling crystallization. Disadvantages of the antisolvent crystallization approach include the higher supersaturation gradients within the solution in larger scale systems, the additional costs associated with the solvent separation, and the larger capital costs required due to the often higher operating volumes. Figure 1 shows the schematic representation of the operating curves for both seeded and unseeded systems for cooling or antisolvent crystallization. The main difference between seeded and unseeded systems is that for the unseeded case the operating curve has to cross the nucleation boundary to generate *in situ* the seed, whereas in the seeded operation crystals with well determined properties are added at small but positive supersaturation. The operating curves are similar conceptually independently whether cooling or antisolvent is used to generate the supersaturation, however the boundaries of the metastable zone change, and the shape of the optimal operating curve can vary significantly.

Several approaches have been proposed for designing the operating curves for crystallization systems. Generally speaking, two main categories can be distinguished, which are schematically depicted in Figure 2. The model-based design approach is based on developing a detailed model which is used with optimization techniques to determine temperature versus time or antisolvent addition rate versus time trajectories (Rawlings et al., 1993). Advantages of the model-based approach include its ability to obtain a theoretically optimal recipe, much smaller number of experiments than for statistical experimental design of batches (Togkalidou et al., 2001b), increased process understanding, and the possibility of incorporating the effects of nonideal mixing via computational fluid dynamics (Woo et al., 2006). Disadvantages associated to the model-based approach are mainly related to the difficulty in modelling practical objectives (e.g., filterability, purity, tablet stability, etc.), and the significant time and engineering effort required for the model development. Additionally, the performance of the model-based approach depends on the model accuracy; the robustness of the approach can be improved by incorporating linear or nonlinear robustness analysis into the optimization (Nagy and Braatz, 2003; 2004).

The model-free (or direct design) approach is based on the understanding of the basic concept of crystallization to operate the system within the metastable zone bounded by the nucleation and solubility curves (see Figure 1). A supersaturation setpoint is followed in the phase diagram using concentration measurement and supersaturation control approaches. This approach also generates experimentally the temperature or antisolvent versus time profiles, which can be implemented at the production scale where the concentration measurement might not be readily available. The main advantage of the direct design technique is that it provides a fast approach for recipe design, which also can be highly automated. It also requires very simple mathematical tools, without any modelling effort. The main disadvantage of the approach is that the operating curve chosen in the phase diagram is not necessarily optimal. Although the close-to-optimal setpoint profile mostly provides very good performance for practical purposes, it is also possible to apply measurement-based optimization approaches (Welz et al., 2004) to improve the initial setpoint profile according to a run-to-run control scheme, leading to an optimal direct design strategy.

Both the direct design and model-based design approaches are based on the fundamental concept that the ideal region for the crystallization operation is within the metastable zone once the nuclei have formed or were introduced via seeding. However, in more modern crystallization designs this concept has been extended, and it has been shown that driving the system into the undersaturated region can yield better crystal quality via controlled fine dissolution (Doki et al., 2004). Controlled *in situ* dissolution is also an

efficient way for adaptive crystallization control, which can correct the effects of changes in operating conditions due to scale-up or disturbances (e.g., variations in seeding). The main idea of the approach is based on *in situ* measurement of the particle counts in the system (e.g., using focused beam reflectance measurement – FBRM), and when excessive increase in the desired number of counts per unit time is detected, dissolution is used to correct the number of counts. Dissolution can be controlled by adding more solvent into the system or increasing the temperature with a predetermined rate, or by applying a control algorithm which determines the degree of dissolution in correlation with the extent of nucleation detected. After the desired number of counts is achieved supersaturation is controlled again by cooling or antisolvent addition or the combination of the two.

3. MATHEMATICAL MODELLING OF COMBINED COOLING AND ANTISOLVENT CRYSTALLIZATION SYSTEM

3.1 Population balance model and solution approach

The population balance for a batch or semibatch system (Randolph and Larson, 1988), when crystals are characterized by one characteristic length and the volume is time-varying, is given by:

$$\frac{\partial(n(L,t)V)}{\partial t}+\frac{\partial(n(L,t)GV)}{\partial L}=BV \qquad (1)$$

where n is the volumetric number density (expressed on the basis of mother liquor), V is the volume of the mother liquor (m^3), G is the growth rate (m/s), L is the characteristic crystal size (m), and B is the total rate of nucleation ($\#/m^3s^{-1}$). The above equation is derived from the generic population balance equation (PBE), assuming that the crystals retain their shape and there is no breakage or aggregation. The working volume of the semibatch system, characteristic to the antisolvent crystallization, is time-varying, therefore it is more convenient to redefine the number density n on the basis of the total volume of the mother liquor of the crystallizer,

$$\tilde{n}(L,t)=n(L,t)V\,. \qquad (2)$$

Substituting (2) into (1) the PBE becomes:

$$\frac{\partial\tilde{n}(L,t)}{\partial t}+\frac{\partial(\tilde{n}(L,t)G)}{\partial L}=BV. \qquad (3)$$

There have been a variety of different approaches proposed to reformulate the population balance model into computationally more affordable forms suitable for optimization. Model reduction based on the fact that the dominant dynamics of the crystallizer can be described by a small number of degrees of freedom

can be applied using the method of moments (Randolph and Larson, 1988). The *j*th moment of the distribution $\tilde{n}(L,t)$ is defined by

$$\tilde{\mu}_j(t) = \int_0^\infty L^j \tilde{n}(L,t)dL, \qquad j = 0,1,\ldots,\infty, \tag{4}$$

where the moment $\tilde{\mu}_j$ is in units of m^j. These moments have physical meaning. For example, $\tilde{\mu}_0$ is the total number, $\tilde{\mu}_1 / \tilde{\mu}_0$ is the average length, $\tilde{\mu}_2$ is proportional to the total surface area, and $\tilde{\mu}_3$ is proportional to the total volume of crystals in the batch. Multiplying the population equation (3) by L^j, and integrating over all crystal sizes, results in an infinite set of ordinary differential equations (ODEs), which describes the rate of change of the moments of the crystal size distribution. Assuming the nuclei have essentially zero size (Randolph and Larson, 1988), the method of moments leads to:

$$\frac{d\tilde{\mu}_0(t)}{dt} = B(t)V(t)\,, \tag{5}$$

$$\frac{d\tilde{\mu}_j(t)}{dt} = j\mu_{j-1}(t)G(t), \quad j = 1,\ldots,\infty\,. \tag{6}$$

The moments $\tilde{\mu}_j$ characterize the total crystal population (crystals grown from seeds as well as new crystals formed through primary nucleation). In order to characterize the distribution of the seed-grown crystals only, the PBE can be written exclusively for the seed, and applying the method of moments yields the additional ODEs (Rawlings et al., 1993):

$$\frac{d\tilde{\mu}_{0,s}(t)}{dt} = 0\,, \tag{7}$$

$$\frac{d\tilde{\mu}_{j,s}(t)}{dt} = j\mu_{j-1}(t)G(t), \quad j = 1,\ldots,\infty\,. \tag{8}$$

The initial conditions $\tilde{\mu}_{j,s} = \tilde{\mu}_j$, since the only nuclei at $t = 0$ are those provided by the seed.

For the lovastatin crystallization system, water is used as the antisolvent, which is added with a flowrate of F_w (g water/min) to the lovastatin solution in an organic solvent (acetone) throughout the batch. Since the variation in the mass of the total solvent mixture (mother liquor) m_{liq} is due to the water addition, the total mass balance for the solvent mixture is written as follows:

$$\frac{dm_{liq}}{dt} = F_w\,. \tag{9}$$

The mass balance on the solute can be written:

$$\frac{d(C_s m_{liq})}{dt} = -3\rho_c k_v \int_0^\infty L^2 G\tilde{n}(L,t)dL \,, \qquad (10)$$

where C_s is the solute concentration in g solute/g solvents, ρ_c is the density of the crystal, and k_v is the volumetric shape factor, which is the volume of a single crystal divided by L^3. Equations (9) and (10) can be combined to give

$$\frac{dC_s}{dt} = -\frac{C_s}{m_{liq}} F_w - 3\rho_c k_v \frac{\tilde{\mu}_2}{m_{liq}} \,. \qquad (11)$$

Similarly, the concentration of the organic solvent (acetone), $C_{acetone}$ (g acetone/g solvents), is given by the component material balance:

$$\frac{dC_{acetone}}{dt} = -\frac{C_{acetone}}{m_{liq}} F_w \,. \qquad (12)$$

The volume of the mother liquor is calculated from the total mass of the solvent $V = m_{liq}/\rho_{liq}$, where the variation in the density of the mother liquor ρ_{liq} is considered through

$$\rho_{liq} = \frac{1}{C_{acetone}/\rho_{acetone} + (1 - C_{acetone})/\rho_w} \,. \qquad (13)$$

3.2 Kinetics of nucleation and growth

There are different empirical and semi-empirical equations in the literature which express the nucleation and growth rate as a function of the supersaturation. For the API studied (lovastatin), the growth rate is expressed by (Randolph and Larson, 1988):

$$G = A_g \exp(-E_g/RT(t))S(t)^g \,, \qquad (14)$$

where S is the logarithm of the relative supersaturation, $S = \ln(C/C^*)$, with C^* the equilibrium concentration. Our simulations will use the growth and nucleation kinetics measured by Mahajan and Kirwan (1994) for this system for a wide range of supersaturations. The kinetic order of crystal growth was measured to be g = 6.7, which is unusually high, which they explained by a polynuclear surface nucleation growth mechanism. The activation energy was measured as 280 kJ/mol. The nucleation expression uses a relationship that connects geometry, surface tension, free energy, and supersaturation ratio

$$B = A_b \exp\left(K_b T(t)^{-3} S(t)^{-2}\right) \,, \qquad (15)$$

where the cumulative constants A_b and K_b combine several system specific parameters, such as geometry, surface tension, and free energy.

3.2 Solubility of lovastatin in the combined antisolvent-cooling system

In the case of combined antisolvent-cooling crystallization, the equilibrium concentration of the solute is a function of both the solvent/antisolvent composition X, and the temperature, T, i.e., $C^* = f_{sol}(X,T)$. Experiments were performed at different acetone/water ratios and different temperatures to determine the equilibrium curve of the lovastatine-water-acetone system, using process analytical technology tools. ATR-FTIR spectroscopy was used to monitor the solution concentrations through the change in the absorbance. The IR spectra measured using the ATR-FTIR probe are a function of the solution concentration, temperature, and solvent/antisolvent ratio (see Fig. 3). Several approaches are available to correlate the solution concentration with the IR spectra. The most accurate results were obtained using calibration approaches based on chemometrics that incorporate absorbances in a range of frequencies rather than the peak absorbance or the area under the peak together with the temperature values (e.g., Togkalidou et al., 2001b). The concentration values obtained from the IR spectra were compared to solubility measurements obtained by high performance liquid chromatography (from Merck). The experimental results in Fig. 4 illustrate the significant nonlinearity of the solubility with respect to variation of the solvent/antisolvent ratio and temperature. The solubility surface was too nonlinear to obtain high quality correlation models using standard linear multivariate regression techniques, such as partial least squares (PLS) or principle component regression (PCR), so the solubility $f_{sol}(X,T)$ was fit to an artificial neural network (ANN) model. The experimental data were used to train several ANNs to identify a topology that avoids overfitting and poor generalization.

The ANN model can be used to calculate the solubility concentration for any given *X* and *T* (see Fig. 5). Since the actual driving force of crystallization is the supersaturation, independently of whether it is generated by antisolvent addition or cooling, the solubility surface shown in Fig. 5 can be used for systematic determination of the conditions under which the process is better controlled by antisolvent addition or by cooling, based on the sensitivity of the solubility with respect to change in solvent/antisolvent ratio or temperature. Point A on Fig. 5, for example, corresponds to a temperature-controlled operating region, since the solubility in this operating region exhibits higher sensitivity to changes in temperature than in anitsolvent concentration. If the operating point is in other region of the solubility surface (e.g., due to different initial concentration), such as point B on Fig. 5, the system exhibits significantly higher sensitivity to changes in the antisolvent concentration.

4. MATERIALS AND EQUIPMENT

Pure lovastatin from an industrial batch were used in all experiments. Deionized water and acetone of laboratory grade were used in all tests. Experiments were performed in a jacketed 500-mL round-bottomed flask. The temperature was measured using a Fluke 80TK Teflon-coated thermocouple module connected to a computer, and it was controlled by ratioing hot and cold water using a research control valve (Badger Meter, Inc.) via a proportional-integral computer control system designed via internal model control. Chord length distributions of lovastatin crystals in solution were obtained using FBRM (Lasentec) connected to a Pentium III running version 6.0b9 of the FBRM Control Interface software. The chord length distributions are closely related to the crystal size distribution (e.g., see Hukkanen and Braatz, 2003, and references cited therein). The IR spectra of the lovastation solution were obtained using a DIPPER-210 ATR immersion probe with two reflections (Axiom Analytical) with ZnSe as the internal reflectance element. The probe was attached to a Nicolet Protégé 460 FTIR spectrophotometer connected to a Pentium II computer running OMNIC 4.1a software from Nicolet Instrument Corp. The spectrophotometer was purged with N_2 gas 1 hour before and while measurements were taken to reduce the effect of CO_2 absorption in its optical path. Temperature readings were collected every 2 seconds and averaged during the collection of each spectra, which consisted of 32 scans (1 min interval). The water used as antisolvent was pumped into the apparatus through L/S 6409-13 tubing by a MasterFlex Console Driver with EasyLoad II peristaltic pump, calibrated before the experiments. A 6-cm oval blade attached to an IKA overhead mixer with a flexible shaft was used to stir the solution. Additionally a Lasentec particle vision measurement (PVM) probe was also introduced in the system for monitoring purposes. The three computers connected to the instruments were supervised by a fourth master computer via a software written in LabVIEW (National Instruments). The experimental setup is shown schematically on Fig. 6.

5. OPTIMAL CONTROL – SIMULATION RESULTS

Using the model in Section 3, the control problem of computing the optimal temperature and antisolvent addition rate profiles is formulated as a nonlinear optimization problem, which was solved using sequential quadratic programming (SQP). A convenient way to describe the optimal trajectories is to discretize the batch time in *N* intervals and consider the temperatures and anitsolvent flow rates at every discrete time $k = 0,\ldots,N$ as the optimization variables. In this case the optimal control problem can be written as follows (similar to the formulation for cooling, see Rawlings et al., 1993):

$$\underset{T(k),\ F_w(k)}{\text{optimize}}\, J\ , \qquad (16)$$

subject to:

$$
\begin{aligned}
&T_{\min} \le T(k) \le T_{\max},\\
&R_{T,\min} \le dT(k)/dt \le R_{T,\max},\\
&F_{w,\min} \le F_w(k) \le F_{w,\max},\\
&C(N) \le C_{\max},\\
&V(N) \le V_{\max},
\end{aligned}
\qquad (17)
$$

where $T_{\min}$, $T_{\max}$, $R_{T,\min}$, and $R_{T,\max}$ are the minimum and maximum temperatures and temperature ramp rates, respectively, and $F_{w,min}$ and $F_{w,max}$ the minimum and maximum flow rates during the batch. The first three constraints ensure that the temperature and antisolvent flowrate profiles stay within the operating range of the crystallizer. The fourth constraint ensures that the solute concentration at the end of the batch C_{final} is smaller then a certain maximum value $C_{final,max}$ set by the minimum yield required by economic considerations, whereas the final constraint limits the total amount of antisolvent, which can be added due to the limit in the capacity of the crystallizer, $V_{\max}$. The objective J is written in terms of some desired characteristic of the crystals at the end of the batch. In this study the following crystal size distribution (CSD) properties were considered: number-average crystal size $J_{n.m.s.} = \mu_1/\mu_0$, coefficient of variation $J_{c.v.} = (\mu_2\mu_0/\mu_1^2 - 1)^{1/2}$, nucleation-to-seed-mass ratio $J_{n.s.r.} = (\mu_3 - \mu_{3,s})/\mu_{3,s}$, and weight-mean size $J_{w.m.s.} = \mu_4/\mu_3$.

The optimization results are in Table 1. For easier comparison normalized values are shown, considering the cooling batch operation as the base case. Antisolvent operation generally provided better performance than cooling batch operation. This is consistent with the analysis of the solubility surface (Fig. 5), which shows generally a higher sensitivity to the antisolvent concentration than to temperature, suggesting the possibility of better control via antisolvent addition than by cooling. The difference in product quality depends on the equilibrium/kinetic model and on the operating constraints. Simulations indicated that, while antisolvent addition provided significantly higher yield for almost all realistic perturbations in the model and constraints, similar product quality can be achieved for cooling and antisolvent addition if the constraints of the optimization problem are relaxed sufficiently. One of the advantages of antisolvent crystallization is that the antisolvent addition rate can be changed much faster than the cooling profile, hence faster response in the supersaturation profile can be achieved. In practice, capacity constraints may limit the maximum performance. Simulations showed that the combined operation offers better performance for all four objective functions, providing the maximum yield for

fixed capacity and operating temperature range. Figure 7 shows a typical cooling profile for the cooling-only crystallization with $J_{n.m.s.}$ as the objective. The overall shape of the profile is similar to many optimal cooling profiles reported in the literature for other systems, favoring higher growth rates later in the batch. For the antisolvent-only system (with objective $J_{n.m.s.}$), a lower initial antisolvent addition rate is observed, which increases as the crystallization progresses, until it reaches its upper limit (Fig. 8). After about 140 min the hard constraint on the crystallizer capacity is met, and the antisolvent addition is stopped. For the combined cooling-antisolvent system, the shapes of the temperature and the antisolvent addition profiles change significantly (Figs. 9 and 10) compared to the individual operating modes. It can be observed that independently whether the objective is to maximize the number-average crystal size (Fig. 9) or minimize the nucleation-to-seed-mass ratio (Fig. 10), in the initial part of the batch is mainly controlled by cooling. This can be explained by the fact that initially at low antisolvent concentration the solubility shows higher sensitivity to temperature changes. During the second half of the process in the first case a combined effect of the antisolvent addition and the cooling is used to control the supersaturation, whereas for the second objective the temperature dropped very fast and the antisolvent addition varied only in the second half of the batch.

6. EXPERIMENTAL RESULTS

The shapes of the optimal profiles for cooling-only, antisolvent-only, and the combined system were also evaluated experimentally both for seeded and unseeded cases, using the experimental setup described in Section 4. The optimal profiles were shortened to a duration of one hour. Figure 11 shows the seed and products obtained in the case of seeded operation. The entire FBRM chord length distribution (CLD) along the batch is shown for the cooling and antisolvent operations in Figs. 12 and 13, respectively. In both systems, significant secondary nucleation was observed shortly after the seed addition. This is most likely due to the application of the operating policies on a shorter timeframe than obtained from simulations, which resulted in faster cooling and antisolvent addition.

For the cooling operation the number of counts increases (Fig. 14), indicating nucleation during the entire duration of the batch, which yields lower average particle size. Figure 14 indicates that for the antisolvent crystallization the total number of counts obtained from the FBRM stays at a relatively constant level for most of the run, which results in significantly larger mean size (Fig. 15). The slight decrease in the number of counts after nucleation until ~0.7 h is due to the effect of dilution on the FBRM probe. After t = 0.7 h, the antisolvent addition was stopped according to the mapped profile and the

number of counts remained constant. The batch with antisolvent addition also resulted in significantly higher yield of crystals. The crystal quality was monitored during the batch using PVM, confirming the results obtained from FBRM data. Figure 16 shows a typical PVM image of lovastatin crystals obtained in the antisolvent addition system. The experimental results indicate that, for the lovastatin system, antisolvent and combined crystallization leads to significantly higher crystal quality and better yield than in the case of the cooling-only system (combined operation can only perform better than antisolvent addition operation). Although the cooling-only crystallization resulted in the poorest crystal size distribution among the seeded crystallizations for this system, it does produce much better crystals than unseeded operations. In the case of unseeded cooling-only operation (see Fig. 1), the large metastable zone width for this system resulted in excessive nucleation, resulting in low quality crystals with small size, wide distribution, low reproducibility, and low yield (see Fig. 17).

While nearly all systems that combine antisolvent addition and cooling crystallization are expected to produce higher quality crystal size distributions than either antisolvent addition-only and cooling-only crystallization, whether antisolvent addition-only or cooling-only operations are preferred from a control point of view for a particular solute-solvent-antisolvent system depends strongly on the shape of the solubility surface (e.g., Fig. 5), as well as on the other considerations described in Section 2.

7. CONCLUSIONS

Strategies that combine antisolvent and cooling operation to control the supersaturation during batch crystallization are developed. The pros and cons of cooling and antisolvent addition strategies are corroborated for a sample API, lovastatin, using simulation and experimental studies. An optimization study indicates that combining the two strategies results in superior control of the crystal size distribution.

ACKNOWLEDGEMENTS

The first author gratefully acknowledges the financial support by EPSRC (EP/E022294/1 and CASE/CAN/06/38). Merck is acknowledged for providing the lovastatin for these experiments.

REFERENCES

Barrett, P., Smith, B., Worlitschek, J., Bracken, V., O'Sullivan, B., O'Grady, D., A review of the use of process analytical technology for the understanding and optimization of production batch crystallization processes. *Organic Process Research & Development*, **9** (2005) 348-355.

Birch, M., Fussell, S.J., Higginson, P.D., McDowall, N., Marziano, I., Towards a PAT-Based strategy for crystallization development. *Organic Process Research & Development* **9** (2005) 360-364.

Braatz, R.D. Advanced control of crystallization processes. *Annual Reviews in Control* **26** (2002) 87-99.

Doki, N., Seki, H., Takano, K., Asatani, H., Yokota, M. and Kubota, N. Process control of seeded batch cooling crystallisation of the metastable alpha-form glycine using an in-situ ATR-FTIR spectrometer and an in-situ FBRM particle counter. *Crystal Growth & Design* **4** (2004) 949-953.

Feng, L.L., Berglund, K.A. ATR-FTIR for determining optimal cooling curves for batch crystallisation of succinic acid. *Crystal Growth & Design* **2** (2002) 449-452.

FDA, U.S. Department of Health and Human Services, Guidance for industry – PAT, http://www.fda.gov/cder/guidance/6419fnl.pdf (2004).

Fujiwara, M., Chow, P.S., Ma, D.L. and Braatz, R.D. Paracetamol crystallisation using laser backscattering and ATR-FTIR spectroscopy: Metastability, agglomeration, and control. *Crystal Growth & Design* **2** (2002) 363-370.

Fujiwara, M., Nagy, Z. K., Chew, J. W., Braatz, R. D., First-principles and direct design approaches for the control of pharmaceutical crystallization. *J. of Process Control* **15** (2005) 493-504.

Hukkanen, E.J., Braatz, R.D. Measurement of particle size distribution in suspension polymerization using in situ laser backscattering. *Sensors & Actuators B* **96** (2003) 451-459.

Jones, A.G. *Crystallization Process Systems*. Butterworth-Heinemann, Oxford, 2002.

Jones, A.G., Teodossiev, N.M. Microcomputer programming of dosage rate during batch precipitation. *Crystal Research & Technology* **23** (1988) 957-966.

Liotta, V., Sabesan, V. Monitoring and feedback control of supersaturation using ATR-FTIR to produce an active pharmaceutical ingredient of a desired crystal size. *Organic Process Research & Development* **8** (2004) 488-494.

Mahajan, A.J., Kirwan, D.J. Nucleation and growth kinetics of biochemicals measured at high supersaturations. *J. of Crystal Growth* **144** (1994) 281-290.

Nagy, Z.K., Braatz, R.D. Robust nonlinear model predictive control of batch processes. *AIChE J.* **49** (2003) 1776-1786.

Nagy, Z.K., Braatz, R.D. Open-loop and closed-loop robust optimal control of batch processes using distributional and worst-case analysis. *J. of Process Control* **14** (2004) 411-422.

Nagy, Z.K., Chew, J.W., Fujiwara, M. Braatz, R.D. Advances in the modeling and control of batch crystallizers. in *Proc. of the 7th IFAC Symp. on Advanced Control of Chemical Processes*, Elsevier Scientific, Oxford, UK (2004) 83-90.

Rawlings, J.B., Miller, S.M., Witkowski, W.R. Model identification and control of solution crystallization processes: A review. *Ind. Eng. Chem. Res.* **32** (1993) 275-1296.

Randolph, A. and Larson, M.A. *Theory of Particulate Process*. 2nd ed. Academic Press, San Diego, 1988.

Togkalidou, T., Braatz, R.D., Johnson, B.K. Davidson, O., Andrews, A., Experimental design and inferential modeling in pharmaceutical crystallization, *AIChE J.* **47** (2001a) 160-168.

Togkalidou, T., Fujiwara, M., Patel, S., Braatz, R.D. Solute concentration prediction using chemometrics and ATR-FTIR spectroscopy. *J. of Crystal Growth* **231** (2001b) 534-543.

Welz, C., Srinivasan, B., Bonvin, D. Combined on-line and run-to-run optimization of batch processes with terminal constraints. in *Proc. of the IFAC Symp. on Advanced Control of Chemical Processes*, Elsevier Scientific, Oxford, UK (2004) 55-62.

Woo, X.Y., Tan, R.B.H., Chow, P.S., Braatz, R.D. Simulation of mixing effects in antisolvent crystallisation using a coupled CFD-PDF-PBE approach. *Crystal Growth & Design* **6** (2006) 1291-1303.

Yu, L. X., Lionberger, R. A., Raw, A. S., D'Costa, R., Wu, H. Q., Hussain, A. S. Applications of process analytical technology to crystallization processes. *Advanced Drug Delivery Reviews* **56** (2004) 349-369.

Zhou, G.X., Fujiwara, M., Woo, X.Y., Rusli, E., Tung, H.H., Starbuck, C., Davidson, O., Ge, Z.H., Braatz, R.D. Direct design of pharmaceutical antisolvent crystallization through concentration control. *Crystal Growth & Design* **6** (2006) 892-898.

Figure Caption

List of Tables

Table 1. Comparison of the three operating modes for different objective functions. Normalized values are used for the objectives using the cooling crystallization as reference.

CSD property	Obj.	Cooling only	Antisolvent only	Cooling + Antisolvent
$J_{n.m.s.}$	max.	1.00	1.15	1.22
$J_{c.v.}$	min.	1.00	0.91	0.86
$J_{n.s.r.}$	min.	1.00	0.83	0.77
$J_{w.m.s.}$	max.	1.00	1.09	1.13

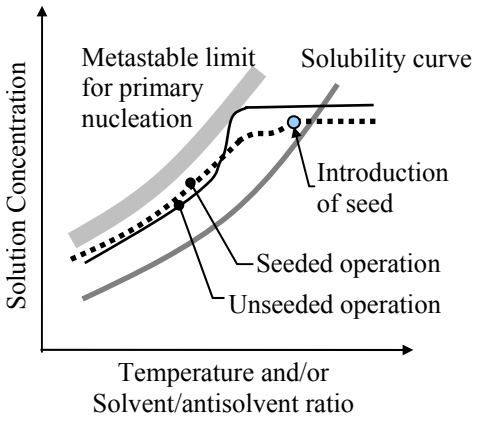

Fig. 1. Operations of seeded and unseeded batch cooling and/or antisolvent crystallizers.

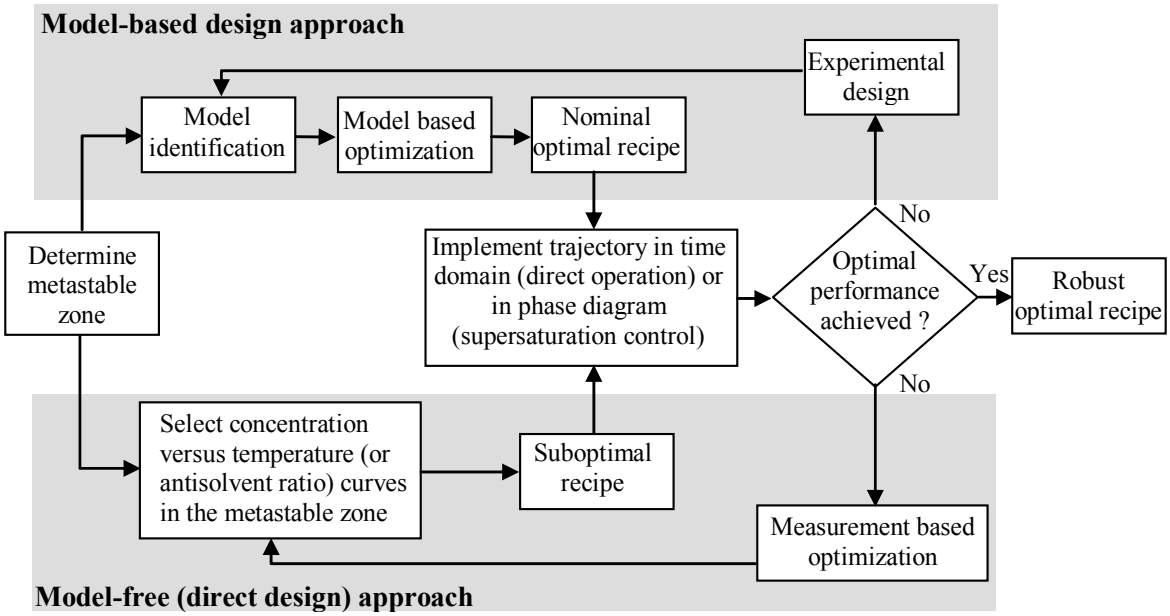

Fig. 2. Schematic representation of the model-based and model-free (direct design) approaches for cooling, antisolvent or combined crystallization systems.

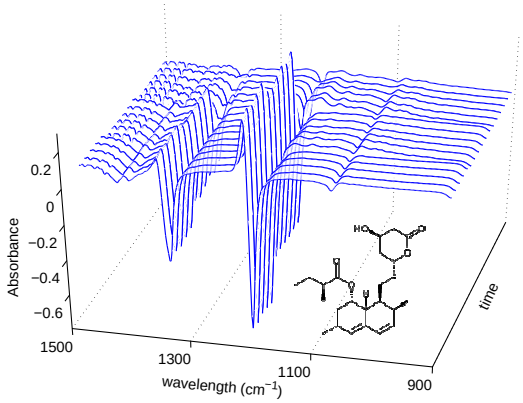

Fig. 3. Molecular formula and IR spectra of lovastatin at different temperatures, concentrations, and solvent/antisolvent ratios.

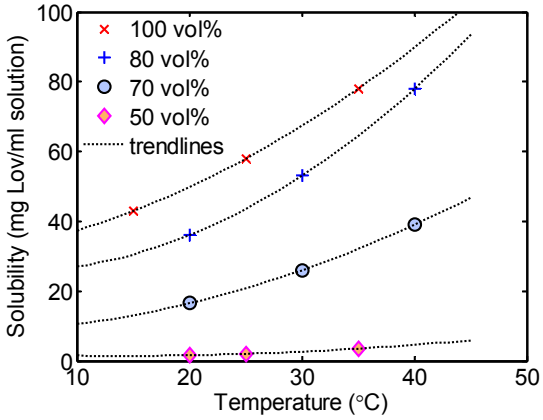

Fig. 4. Solubility curves of lovastatin at different acetone concentrations.

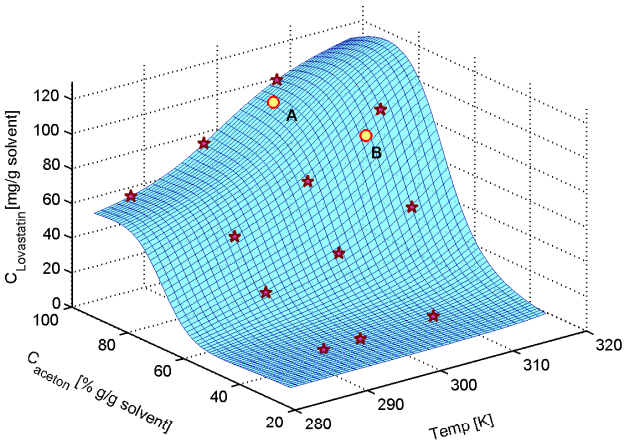

Fig. 5. Solubility surface of lovastatin in acetone/water mixture, obtained from the ANN model. The stars represent the experimental concentrations obtained from the IR spectra. Point **A** indicates high sensitivity for temperature change and low sensitivity for change in antisolvent concentration, whereas point **B** shows high sensitivity for change in antisolvent concentration.

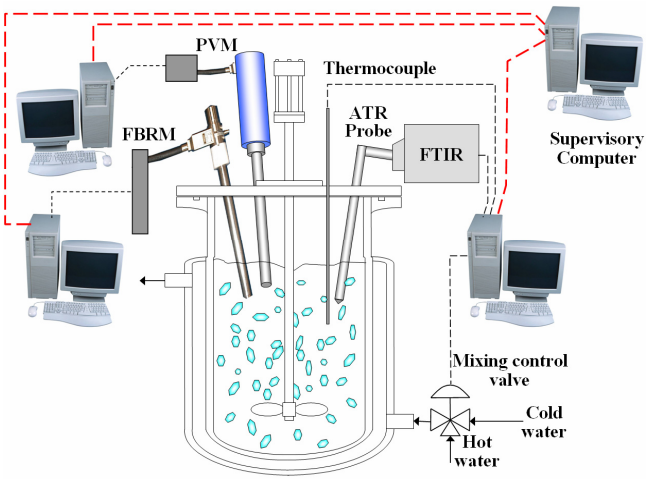

Fig. 6. Schematic representation of the equipment (not drawn to scale).

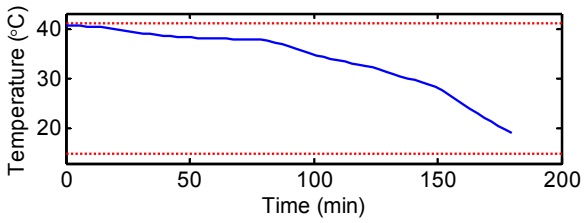

Fig. 7. Optimal temperature profile for cooling crystallization with objective $J_{n.m.s}$.

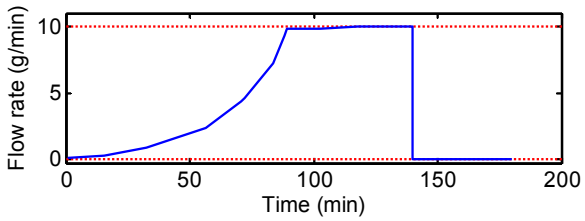

Fig. 8. Optimal flowrate profile for antisolvent crystallization with objective $J_{n.m.s}$.

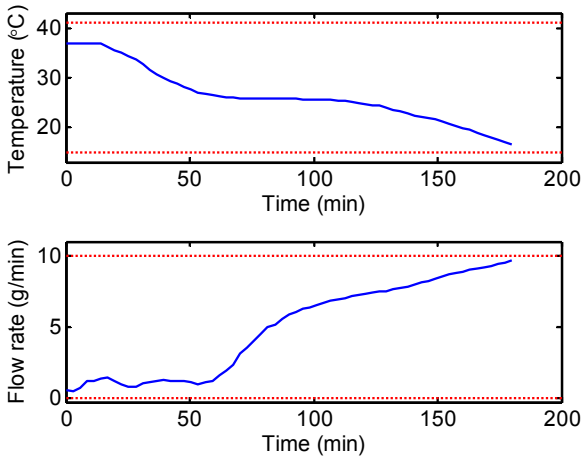

Fig. 9. Optimal operating curves for the combined crystallization with objective $J_{n.m.s}$.

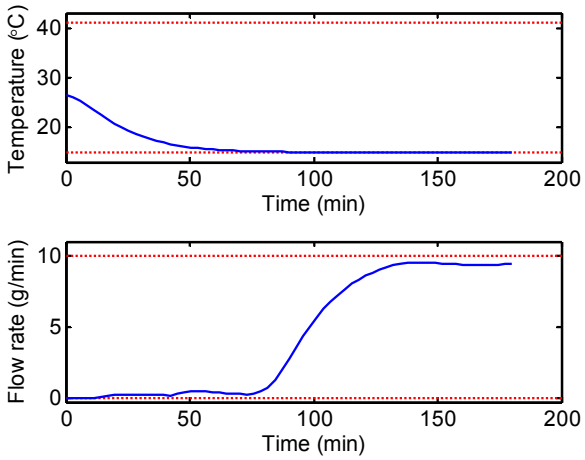

Fig. 10. Optimal operating curves for the combined crystallization with objective $J_{n.s.r.}$.

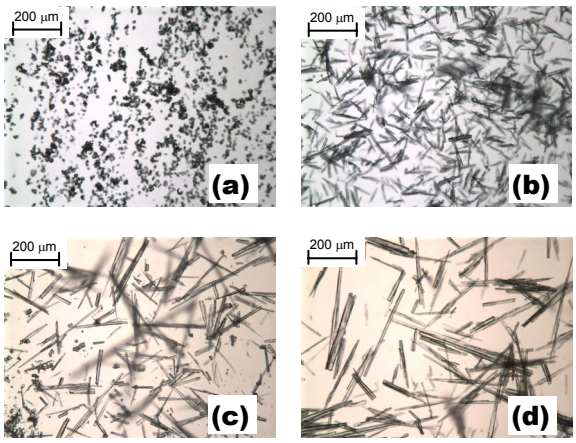

Fig. 11. Microscopic images of seed (a) and product crystals for the three operating modes: (b) cooling-only; (c) antisolvent-only, and (d) combined.

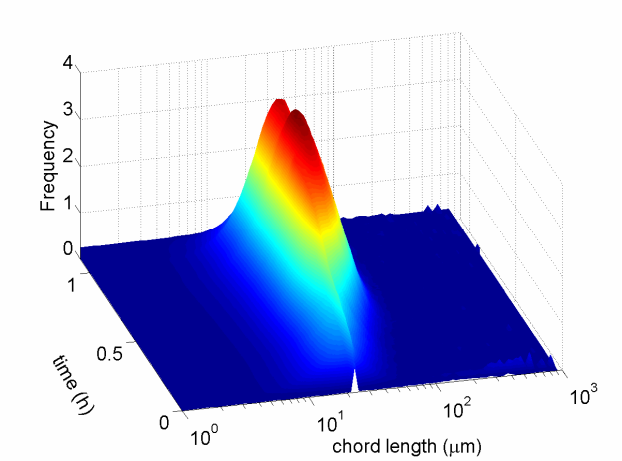

Fig. 12. FBRM CLD for the cooling-only system.

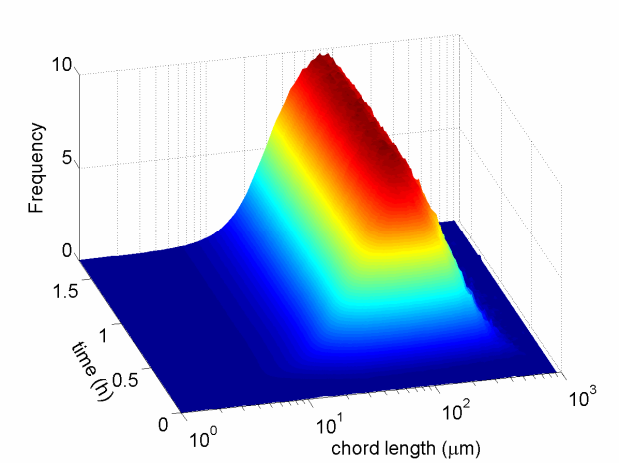

Fig. 13. FBRM CLD for the antisolvent system.

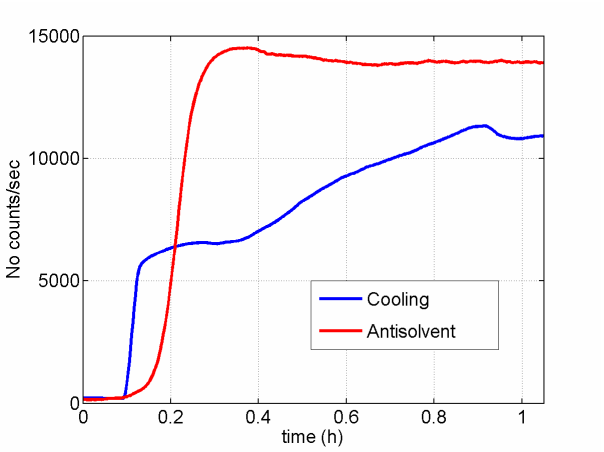

Fig. 14. Total number of counts from FBRM.

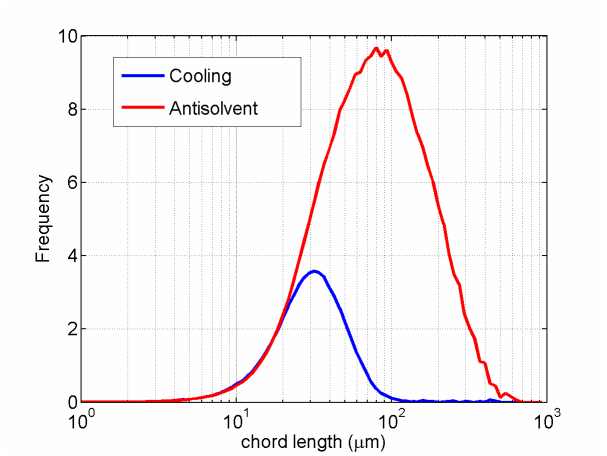

Fig. 15. CLD at the end of the batch for the cooling and antisolvent systems.

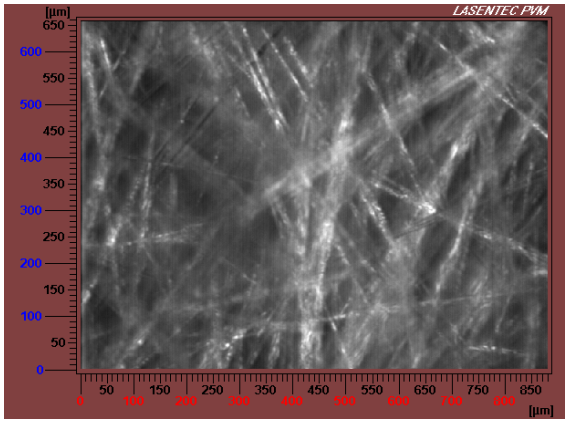

Fig. 16. PVM image of lovastatin crystals.

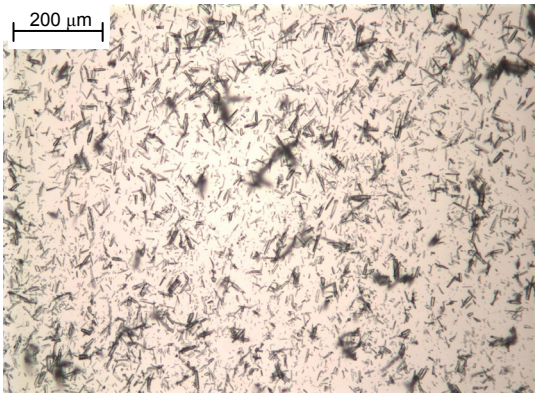

Fig. 17. Lovastatin crystals resulted from the unseeded cooling-only crystallization.